Front. Phys. 13(1), 138204 (2018)
https://doi.org/10.1007/s11467-017-0700-z

RESEARCH ARTICLE

Signature of the hydrogen-bonded environment of liquid water in X-ray emission spectra from first-principles calculations

Huaze Shen[1,2], Mohan Chen[2], Zhaoru Sun[2], Limei Xu[1], Enge Wang[1,†], Xifan Wu[2,3,‡]

[1] *International Centre for Quantum Materials and School of Physics, Peking University, Beijing 100871, China*
[2] *Department of Physics, Temple University, Philadelphia, PA 19122, USA*
[3] *Institute for Computational Molecular Science, Temple University, Philadelphia, PA 19122, USA*
Corresponding authors. E-mail: † egwang@pku.edu.cn, ‡ xifanwu@temple.edu
Received May 15, 2017; accepted June 24, 2017

Based on *ab initio* molecular dynamics simulations and density functional theory, we performed a systematic theoretical study to elucidate the correlation between the H-bonded environment and X-ray emission spectra of liquid water. The spectra generated from excited water molecules embedded in an intact H-bonded environment yield broader spectral peaks and a larger spectral range than the spectra generated from water molecules in a broken H-bonded environment. Such differences are caused by the local electronic structures on the excited water molecules within the core-hole lifetime that evolve differently through the rearrangement of neighboring water molecules in different H-bonded environments.

Keywords water, density functional theory, *ab initio* molecular dynamics, X-ray emission spectra, hydrogen bond, core hole

PACS numbers 61.25.Em, 61.05.cj, 71.15.Pd, 82.30.Rs, 31.15.es

1 Introduction

The fundamental understanding of the structure of liquid water has attracted active investigations using joint experimental and theoretical techniques [1–4]. Although the chemical composition of a water molecule is very simple, the structure of water in condensed liquid is very complicated, particularly the nature of hydrogen bonds (H-bonds) in liquid water, which is still under intense debate [1, 5–27]. The long-standing controversy is partially due to the weak H-bond, which is the key physical interaction that determines the structure of liquid water. Diffraction-based experimental techniques, including neutron diffraction [6, 28–34] and X-ray diffraction [6, 7, 34–39] measurements have been powerful tools for detecting the H-bonded network. However, these diffraction measurements only provide averaged structural information, such as radial distribution functions [34], over a large spatial and temporal scale, which cannot capture the frequent breaking and reforming of H-bonds caused by thermal fluctuations within 1–2 ps [5, 40–47]. Therefore, the local fluctuations of the H-bond network on the femtosecond timescale cannot be sensitively detected by diffraction measurements.

Oxygen K-edge X-ray spectroscopy techniques, including X-ray absorption spectroscopy (XAS) [48–62] and X-ray emission spectroscopy (XES) [8, 48, 61, 63–70] are important to locally probe the H-bond network of liquid water. In XAS, the core 1*s* electrons of oxygen are excited to conduction bands. The excited electrons in the conduction bands are then probed for only the selected *p*-character orbitals. Three main features are observed in the XAS spectra, i.e., pre-edge, main-edge, and post-edge features. The electronic excitations of different edges have distinct spatial localization properties and excitation energies. Specifically, the pre-edge, main-edge, and post-edge features with increasing excitation energies are sensitive to short-, intermediate-, and long-range orderings of the H-bond network, respectively [71]. Complementary to XAS, XES has recently emerged as another useful local probe of the H-bond network. XES can be roughly considered an inverse process of XAS. Unlike

*Special Topic: Water and Water Systems (Eds. F. Mallamace, R. Car, and Limei Xu).

probing the unoccupied states in XAS, the electrons on the occupied states from the excited water molecule return to the core-hole states and emit photons during the X-ray emission process. Compared to the electronic process of XAS, which is well approximated by a frozen core hole, the core-hole-induced molecular dynamics around the excited water must be considered in XES. This is because the core hole has a relatively long lifetime of ~ 3.6 fs [65, 72–74], during which the rearrangement of molecules and their effects on the electronic structure cannot be neglected. Therefore, the core-hole dynamics in XES provides a unique and insightful analysis of the structure of the H-bond network, which is absent in XAS.

Given the molecular structure of liquid water and the core-hole dynamics modeled by *ab initio* molecular dynamics (AIMD) simulations [75], the XES scattering cross section can be computed by the transition matrices of the occupied defect states and the $1s$ core-hole state [65] according to the Fermi golden rule, which is based on the dipole approximation. Along this line, three electronic states, $1b_1$, $1b_2$, and $3a_1$, with oxygen $2p$ character are assigned to the XES spectra based on the selection rule. Compared to the XES spectra of gaseous water with three sharp peaks, the XES spectra of liquid water have broader $1b_2$ and $3a_1$ peaks with relatively narrower lone pair peaks. The spectral difference for gaseous and liquid water has been theoretically predicted [63–65, 67, 69, 75, 76]. The computed spectra were in qualitative agreement with the experiment [8, 48, 61, 64–66, 68–70, 77], indicating the importance of the H-bond network in understanding the XES. Despite significant progress in the field, the influence of fluctuations of the H-bond network in liquid water on the spectra has been much less investigated and discussed.

To address the above issue, we performed a systematic investigation on the electronic structure to study how the H-bonded environment affects the XES spectra through core-hole dynamics. In particular, the XES spectra were decomposed according to different H-bonded environments in liquid water. For excited water molecules embedded in an intact H-bonded environment, we found that the spectra are strongly affected by rapid core-hole dynamics, as evidenced by elongation of the O–H covalent bond. The elongation of the O–H covalent bond delocalizes the defect-like states, leading to an increase in the corresponding energy levels and broad spectra. For excited water molecules embedded in a broken H-bonded environment, the core-hole dynamics can be essentially neglected for a time scale that is comparable to the core-hole lifetime. The O–H covalent bond of the excited water is slightly elongated during the core-hole dynamics, and the changes of its electronic structure can also be neglected. Therefore, the resulting spectral peaks are relatively narrow and sharp. Our calculations and analysis elucidated the relation between the observed XES spectra of liquid water and its underlying H-bond network.

2 Methods

The water simulations were performed using density functional theory [78, 79]. All simulations were performed in the Quantum ESPRESSO [80] package using the Perdew–Burke–Ernzerhof [79] functional and a 72-Ry kinetic-energy cutoff for the plane-wave expansion of the Kohn–Sham wave functions. The ion-electron interactions of deuterium and oxygen atoms were represented by norm-conserving pseudopotentials (NCPP) [81–83]. The NCPP of the oxygen atom with a $1s$ core hole was generated by an oxygen atom with a fully relaxed $1s$ core hole as a reference state. A water system with 64 H_2O molecules was adopted in a cubic cell of size $L = 12.4$ Å with periodic boundary conditions. Note that for gaseous water, we used the same cell size containing one water molecule.

We performed AIMD simulations [14] at 330 K using a constant-temperature, constant-volume ensemble. An extra 30 K was applied to mimic the nuclear quantum effect [84]. We utilized the Nosé–Hoover chain thermostats [85–87] with a chain length of four to control the temperature. The equation of motion in our AIMD simulations was integrated using the standard Verlet algorithm with a time step of 0.1 fs. We used a fictitious mass of 300 a.u. for the electrons. The trajectory was run for 27 ps. The masses for oxygen and hydrogen were 15.9994 and 2.01355 amu, respectively.

We also examined the core-hole dynamics by utilizing the AIMD method. A snapshot of liquid water was chosen from the AIMD simulations as the starting geometry for the core-hole dynamics simulation. Specifically, we first substituted one oxygen atom with an excited oxygen atom before the core-hole dynamics and computed the ground state of this geometry. We then performed a core-hole dynamics simulation with the precalculated ground state and the velocities chosen from the selected snapshot. Note that the same procedures were repeated for all 64 water molecules using one excited water molecule each time. For each AIMD trajectory, a short timescale of 10 fs was used with a time step of 0.5 fs. Using Chandler's H-bond definition [88], we found one water molecule with zero donating H-bonds (0D), ten water molecules with one donating H-bond (1D), and the remaining 53 water molecules with two donating H-bonds (2D) in the selected snapshot. The percentage of broken H-bonds was 9.375%.

The theoretical XES spectra were computed based on

the core-hole dynamics trajectories. We calculated the XES spectra of water for each configuration at different time steps by computing the cross section based on Fermi's golden rule within the electric dipole approximation:

$$\sigma(\omega) = 4\pi^2\alpha_0 \sum_i \hbar\omega |M_{if}|^2 \sigma(\omega - \omega_{if}),$$

where α_0 is the fine structure constant and $\hbar\omega$ is the emitted photon energy that matches the energy difference $\hbar\omega_{if} = |E_i - E_f|$ between the initial and final states. E_i and E_f are the eigenvalues of the initial and final states, respectively. M_{if} is the transition matrix element between the initial and final states, where we take the O 1s atomic orbital as the initial state, $|i\rangle$, and the occupied orbitals as the final state, $|f\rangle$. Only electrons in orbitals with p-character can fill the core hole of the O 1s orbital because of the selection rule; therefore, only the bonding orbitals ($1b_2$ and $3a_1$) and the non-bonding orbital (lone-pair) $1b_1$ can be recorded by XES. The calculated discretized spectra were convoluted with a Gaussian function (0.4 eV) and weighted according to an exponential decay mechanism. An exponential averaging of the XES spectra along the core-hole dynamics trajectory with a lifetime of 3.6 fs was applied.

3 Results and discussion

We present the computed XES spectra of the gas and liquid phases of water in Figs. 1(a) and (b), respectively. We adopt the convention to align the first peak of the theoretical spectra at the same position as that of the experimental value (520.9 eV). The theoretical XES spectra qualitatively agree with the experimental measurements [8, 77]. In particular, the XES spectrum of water vapor can be identified by three distinct peaks centered at 520.9, 523.7, and 525.1 eV with the overall spectrum spanning approximately 7 eV. The three features can be explicitly assigned to three occupied electronic orbitals with $1b_2$, $3a_1$, and $1b_1$ characters, respectively, as a function of increasing energy. The XES spectrum of liquid water also has three major features with the same orbital characteristics as those of gaseous water. However, the XES spectrum of liquid water contains broader features than those of gaseous water and exhibits an overall broader distribution spanning approximately 11 eV. In particular, the peaks associated with $1b_2$ and $3a_1$ characteristics in liquid water are broader than gaseous water. Importantly, the liquid water molecules are embedded in an H-bond network, which is completely absent in the vapor phase. Therefore, the spectral differences between vapor and liquid water suggest that the local electronic states with $1b_2$, $3a_1$, and $1b_1$ characters are nontrivially affected by the fluctuating H-bond interactions of liquid water during the core-hole lifetime.

The rearrangement of the local H-bonded structure around the excited water molecules through core-hole dynamics needs to be considered in the XES process because the time scale of XES is several femtoseconds. To capture the changes of the electronic structures during the core-hole dynamics, we compared the density of states (DOS) of an excited water molecule at $t = 0$ and 3 fs (a time scale that is close to the estimated lifetime of a core-hole of 3.6 fs [65, 72–74]). Figures 2(a) and (b) display the DOS results for both gaseous and liquid water, respectively, with a focus on only the excited water molecule. We find that the energy levels at $t = 0$ and 3 fs are almost unchanged, indicating that the orbitals associated with the three occupied electron levels are almost intact. This is consistent with the observed sharp peaks of the XES from gaseous water in Fig. 1(a). In contrast, the three defect-like states in liquid water are localized on the excited water molecule because of the attractive po-

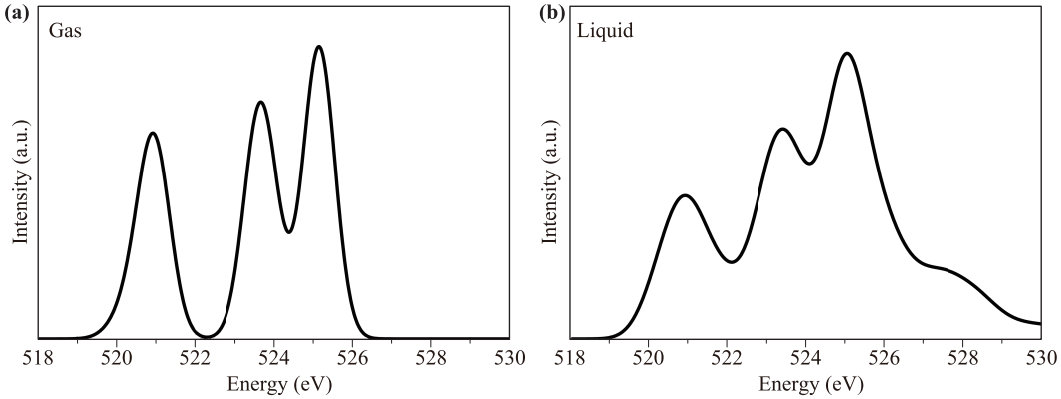

Fig. 1 General features of the computed XES spectra of gaseous water **(a)** and liquid water **(b)**. Both spectra exhibit three peaks corresponding to three occupied molecular orbitals: $1b_2$, $3a_1$, and $1b_1$. The $1b_2$ and $3a_1$ orbitals are bonding orbitals related to O–H bonds, while the $1b_1$ orbital is a non-bonding orbital associated with the lone-pair electrons of oxygen. The peaks of gaseous water are sharper than liquid water because of the H-bonds in liquid water.

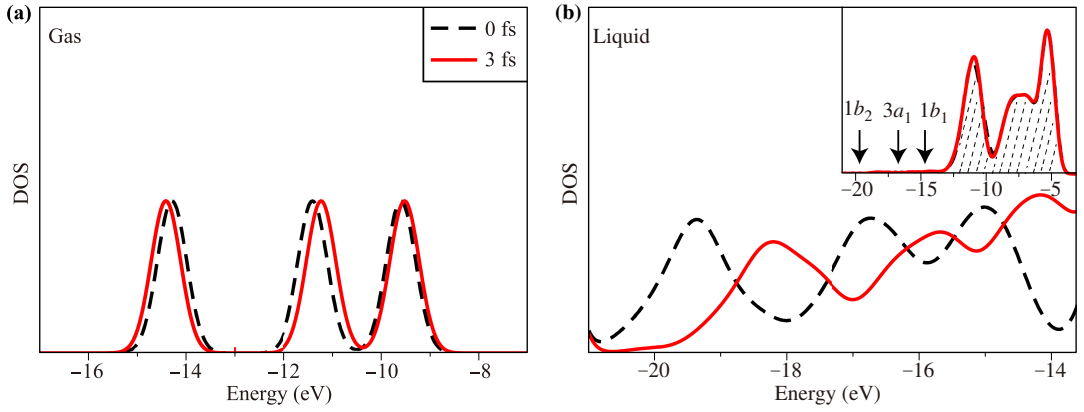

Fig. 2 Computed density of states (DOS) of gaseous water **(a)** and liquid water **(b)** at different times in the core-hole dynamics. The DOS of an excited water molecule in the gas phase exhibits three distinct peaks centered at −14.3, −11.4, and −9.6 eV at time $t = 0$ fs and −14.4, −11.2, and −9.5 eV at $t = 3$ fs. The three peaks are assigned with $1b_2$, $3a_1$, and $1b_1$ characteristics, respectively. No significant change is observed in the DOS of gaseous water at different times in the core-hole dynamics. In contrast, the DOS of liquid water with one excited water molecule exhibits three large peaks (shadowed) and three small peaks (shown with three downward arrows, representing the DOS of $1b_2$, $3a_1$, and $1b_1$ of the excited water molecule, respectively), as depicted in the inset of (b). The three large peaks represent the DOS of 63 ordinary water molecules in the background, while the small peaks correspond to the DOS of the excited water molecule. The DOS associated with the excited water molecule is illustrated in the main figure of (b). The positions of the small peaks at $t = 0$ fs undergo a dramatic shift at $t = 3$ fs, indicating strong influences of the H-bonds on the DOS.

tential from the positive core hole. The inset of Fig. 2(b) displays the total DOS of the liquid water, in which the three small peaks are the defect-like states originating from the excited water molecules in the liquid phase, and the three large peaks occupy the p states from the remaining 63 non-excited water molecules in the system. We find that the three small peaks are located below the oxygen $2p$ bands of DOS and are contributed by the remaining 63 non-excited water molecules. The energy of the DOS for the defect-like states of an excited water molecule in liquid water dramatically changes during the core-hole dynamics, resulting in a broader distribution than that in the gas phase. Furthermore, the energy levels of the excited molecule in liquid water also undergo a blue shift by the observed increased excitation energies as a function of time. As a result, the excited energy levels in liquid water are closer to the electronic states of liquid water, i.e., the three large peaks of the overall DOS. This suggests that the H-bonded network has a dramatic effect on the defect-like states and the electronic orbitals localized on the excited water molecules in the condensed liquid phase.

The effect of the core-hole dynamics can be further illustrated by the O–H covalent bond length of the excited water molecules as a function of time. For an individual water molecule in the H-bond network in the liquid phase, the H-bond network is under constant thermal fluctuation. Therefore, we list two cases for O–H covalent bond lengths in liquid water and compare them to the O–H covalent bond length of water in the gas phase. In the first case, a water molecule is embedded in a perfectly H-bonded local structure of liquid water defined by accepting two and donating two H-bonds; in the second case, a water molecule is in a broken H-bonded environment. Only the donated H-bonds are crucial for the core-hole dynamics; therefore, the perfect and broken H-bonds considered in this study reflect the H-bonded environment of the donated H-bonds. We note that a gaseous water molecule is isolated in the absence of H-bond interactions. Figure 3 shows that the O–H bonds in a perfect H-bonded network undergo a much more prominent elongation than those in a broken H-bonded environment. Specifically, the average O–H bond length in a perfect H-bond network is elongated from 1.00 Å to approximately 1.23 Å within 10 fs. In contrast, the O–H bond lengths in gaseous water and a broken H-bonded environment remain essentially unchanged (∼ 1 Å) during the 10-fs core-hole dynamics.

A core hole created by the X-ray emission leaves the oxygen positively charged, creating a core hole with a strongly attractive potential. Therefore, the electronic structure promptly relaxes to its ground state well before the molecular structure can respond. Accordingly, the three occupied states of excited oxygen transition from the valence bands into the gap between the oxygen $2s$ and $2p$ bands of liquid water, as shown in Fig. 2(b). Simultaneously, this positive core hole exerts extra repulsive forces on the two covalently bonded hydrogen atoms of the excited water molecule. As shown in Fig. 3, the core-hole potential introduces additional rearrange-

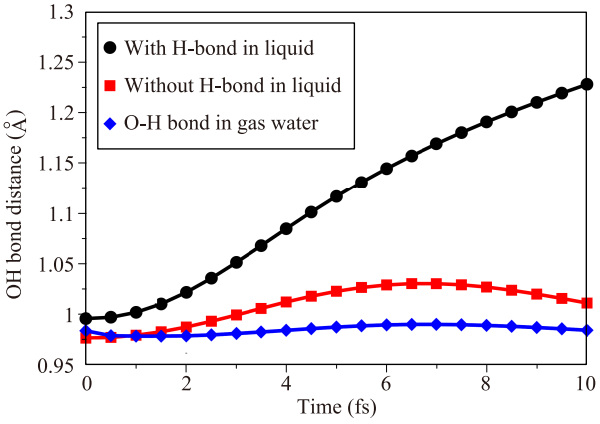

Fig. 3 Length of the covalent O–H bond of the excited water molecule in the gas and liquid phases of water as a function of time during the core-hole dynamics. The O–H covalent bond does not elongate with time for gaseous water. However, for liquid water, when the O–H covalent bond is connected by a H-bond, its length is elongated and the elongation is facilitated by the H-bond. In contrast, for an O–H covalent bond without H-bonds, there is no significant enlargement of the covalent bond length with time. This indicates that the H-bonds significantly affect the core-hole dynamics.

ment of the local molecular structure with a tendency to dissociate the hydrogen atoms from the O–H covalent bonds, which is the process captured by the core-hole dynamics within 10 fs. Figure 3 also shows that the core-hole potential has only a small influence on the hydrogen atoms without the H-bonds in gaseous water or the broken H-bonded environment in liquid water,. However, the above tendency to dissociate protons has been greatly facilitated by connected H-bonds, evidenced by the fast elongation of the O–H covalent bond when the excited water molecule donates H-bonds to its nearby water molecules. The elongation of the O–H covalent bond affects the electronic structure, as captured by the different DOS values of the excited water molecule in the vapor and liquid phases, as shown in Fig. 2.

To study how the core-hole dynamics in different H-bonded environments affects the XES spectra, we further decomposed the spectra into different H-bonded environments. Figures 4(a) and (b) display the XES for excited water molecules in liquid water with zero and two donated H-bonds, denoted as 0D and 2D to represent broken and intact H-bonded environments, respectively. In addition, Figs. 5(a) and (b) illustrate the transition amplitudes computed from the Fermi golden rule for excited water molecules in liquid water with 0D and 2D H-bonded environments, respectively. We further confirm that different H-bonded environments for the excited water molecule in the liquid phase strongly affect the core-hole dynamics, resulting in substantially different shapes in the spectra. The spectra of the excited water in a broken H-bonded network (0D) of liquid water show the least changes during the core-hole dynamics, as shown in Fig. 4(a). Due to the slow core-hole dynamics, the energy levels of the three defect-like states remain almost intact. This is further evidenced by the three very well localized and distinct orbitals with p-characters in Fig. 4(c); these orbitals undergo negligible changes from $t = 0 - 4$ fs. Accordingly, the transition amplitudes illustrated in Fig. 5(a) barely change with time. Moreover, the transition amplitudes follow the relation of $1b_1 > 3a_1 > 1b_2$, which is consistent with the peak intensities in the XES spectra of liquid water.

The spectra from the intact H-bonded (2D) excited water molecules show very different changes during the core-hole dynamics, as illustrated in Fig. 4(b). The core hole with a positive charge is screened during the core-hole dynamics because of the rearrangement of surrounding water molecules, resulting in a less positive environment. Consistently, the three energy levels of the defect-like states within the gap of $2s$ and $2p$ bands of liquid water also continue to increase as a function of time. However, these three orbitals undergo different changes. Firstly, the core-hole dynamics encourages hybridization of the $1b_1$ orbital of the excited oxygen and the $1b_2$ orbitals of the surrounding water molecules along the elongation direction of the O–H covalent bond on the excited water molecule, as shown in Fig. 4(d). The hybridization decreases the transition amplitudes of the spectra, as shown in Fig. 5(b). Meanwhile, Fig. 5(b) further suggests that the resonant states on the neighboring water molecules also increase the number of states that contribute to the optical emission transitions. As a result, the $1b_1$ feature of the XES remains prominent with slightly broadened spectral widths, as shown in Fig. 4(b). Secondly, unlike the strong hybridization of the $1b_1$ state with the surrounding water molecules, the $3a_1$ state on the excited water with a relatively lower energy remains localized. The elongation of the O–H covalent bond stretches the $3a_1$ orbital along the direction of elongation. Consequently, the $3a_1$ orbital becomes more delocalized, resulting in a smaller transition amplitude in Fig. 5(b) and a less prominent spectral feature in Fig. 4(b). Thirdly, the $1b_2$ state of the excited water molecule has the lowest energy with an even more localized orbital at $t = 0$ fs. Similar to that of the $3a_1$ state, the $1b_2$ state is also stretched along the elongation direction of the O–H covalent bond and becomes slightly more delocalized. Therefore, the transition amplitudes are slightly smaller, as shown in Fig. 5(b). Consistently, a less prominent $1b_2$ feature is observed in Fig. 4(b).

After separate discussions of the XES spectra of excited water molecules with 0D and 2D H-bonded envi-

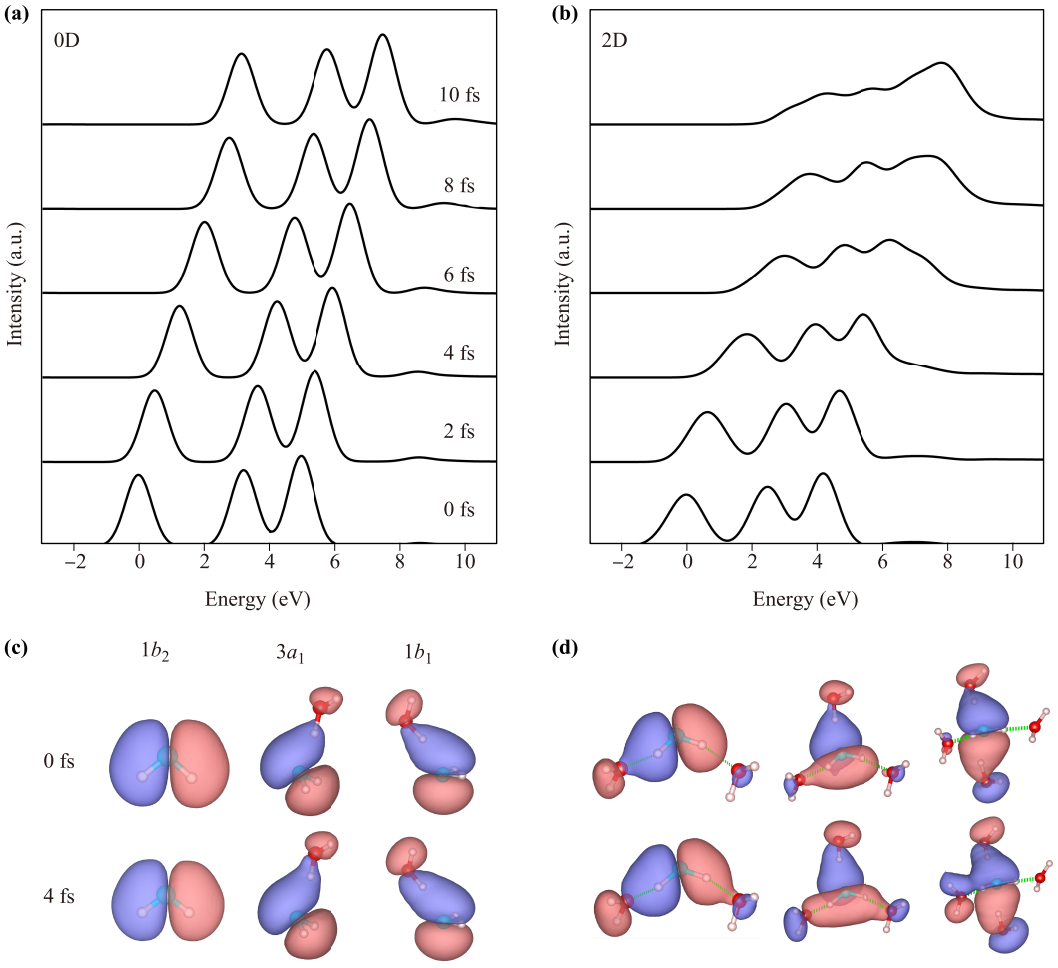

Fig. 4 XES **(a, b)** and orbital graphs **(c, d)** of the excited water molecule in liquid water donating different numbers of H-bonds at different times of the core-hole dynamics. Peaks in the spectra in (a) and corresponding orbitals in (c) are essentially unchanged in the 10-fs core-hole dynamics for the excited water molecule that does not donate any H-bonds. The spectral peaks in (b) become much weaker and broader at a longer time for water molecules donating two H-bonds. Accordingly, the shapes of the corresponding orbitals in (d) significantly stretch and delocalize with time. The excited oxygen atom is depicted in cyan and ground-state oxygen atoms are depicted in red; all hydrogen atoms are shown in white. The H-bonds shown in (d) are highlighted in green.

ronments, we show the overall XES spectra from the two environments in Fig 6. The XES peaks of the excited water molecule embedded in an intact H-bonded environment (2D) are broader than gaseous water [Fig. 1(a))]. Moreover, the energy separation between the different spectral peaks is smaller in the spectra of excited water with 2D than that of water vapor. Both results highlight the important effects of the H-bond network on the XES spectra of liquid water. However, the excited water molecules in an environment with broken H bonds (0D) yield XES spectra that are roughly the same as those of water vapor. The three spectral peaks are less broadened compared to those of excited water molecules with 2D.

In our AIMD simulations, we find that the liquid water structure has a slightly disordered tetrahedral H-bond network with about 9.375% broken H-bonds, which is consistent with the neutron and X-ray diffraction experiments. Therefore, we conclude that the overall computed spectra are strongly affected by the H-bond network, which results in the qualitative spectral differences between the vapor and liquid phases of water. The qualitative consistency between the theory and experiments also supports the near-tetrahedral H-bond network of liquid water.

4 Summary

By using the AIMD simulations, we studied the XES spectra of water and investigated its correlation with the

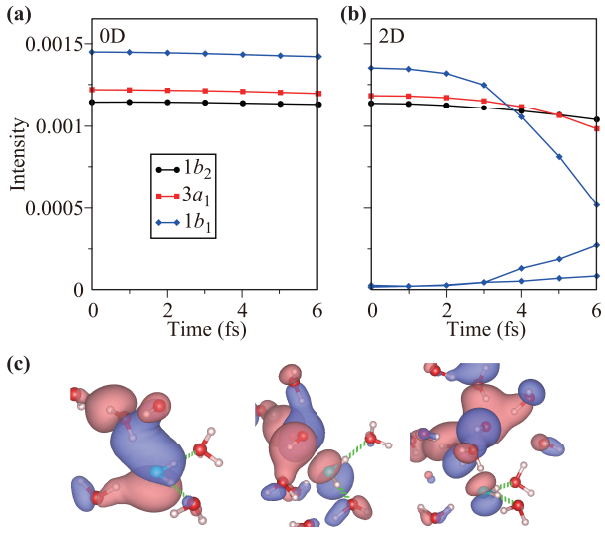

Fig. 5 **(a, b)** The averaged intensities of transition matrices with p-character of $1b_2$, $3a_1$, and $1b_1$ orbitals for excited water molecules donating zero and two H-bonds, respectively. **(c)** The $1b_1$-like orbitals of a representative excited water molecule donating two H-bonds at $t = 4$ fs. Only one orbital contributes to the p-character of $1b_2$ or $3a_1$. However, several orbitals contribute to the $1b_1$ p-character of the excited water molecule at a longer time.

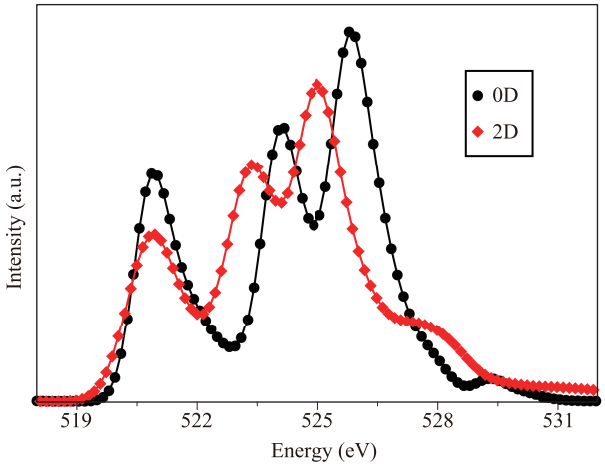

Fig. 6 Computed XES spectra of water embedded in broken (0D) and intact (2D) H-bonded networks in liquid water. The XES spectra of the water molecules in the broken H-bonded environments have less broadened peaks than those in the spectra of water molecules in the intact H-bonded environments.

H-bonds through the electronic structures. The calculated spectra reproduce the main features observed in the experiments, which exhibit three peaks associated with the three occupied orbitals of the excited water molecule. Our study also showed that the spectra are very sensitive to subtle changes in the local environment of the H-bonds, especially the number of donating H-bonds. By analyzing the core-hole-induced dynamics, we observed that the dissociation process of O–H covalent bonds of excited water molecule is fast in the presence of donating H-bonds. The dissociation process further affects the electronic structure (e.g., shape of molecular orbitals and DOS), which can be reflected in the spectra through the core-hole dynamics. In conclusion, our results provide an interpretation of the spectra in terms of the H-bonded network in liquid water. The current simulation is qualitatively consistent with the experimental spectral features. In future studies, more sophisticated and computationally expensive approaches should be adopted to model the XES of liquid water more accurately. For instance, the Bethe–Salpeter equation can be used by also considering the bound excitons in the electronic excited states.

Acknowledgements We acknowledge the National Science Foundation (NSF), DMR under Award DMR-1552287. We also acknowledge the financial support by the National Key Research and Development Program of China (Grant No. 2016YFA0300901) and the National Natural Science Foundation of China (Grant Nos. 11525520 and 11290162). This research used computational resources of the National Energy Research Scientific Computing Center (NERSC), a Department of Energy (DOE) Office of Science User Facility supported by the Office of Science of the U.S. Department of Energy under Contract No. DE-AC02-05CH11231.

References and notes

1. P. Gallo, K. Amann-Winkel, C. A. Angell, M. A. Anisimov, F. Caupin, C. Chakravarty, E. Lascaris, T. Loerting, A. Z. Panagiotopoulos, J. Russo, J. A. Sellberg, H. E. Stanley, H. Tanaka, C. Vega, L. Xu, and L. G. M. Pettersson, Water: A tale of two liquids, *Chem. Rev.* 116(13), 7463 (2016)
2. L. G. M. Pettersson, R. H. Henchman, and A. Nilsson, Water – The most anomalous liquid, *Chem. Rev.* 116(13), 7459 (2016)
3. P. Ball, Water as an active constituent in cell biology, *Chem. Rev.* 108(1), 74 (2008)
4. J. C. Palmer, F. Martelli, Y. Liu, R. Car, A. Z. Panagiotopoulos, and P. G. Debenedetti, Metastable liquid-liquid transition in a molecular model of water, *Nature* 510(7505), 385 (2014)
5. C. J. Fecko, J. D. Eaves, J. J. Loparo, A. Tokmakoff, and P. L. Geissler, Ultrafast hydrogen-bond dynamics in the infrared spectroscopy of water, *Science* 301(5640), 1698 (2003)
6. T. Head-Gordon and G. Hura, Water structure from scattering experiments and simulation, *Chem. Rev.* 102(8), 2651 (2002)

7. J. A. Sellberg, C. Huang, T. A. McQueen, N. D. Loh, H. Laksmono, et al., Ultrafast X-ray probing of water structure below the homogeneous ice nucleation temperature, *Nature* 510(7505), 381 (2014)
8. T. Tokushima, Y. Harada, O. Takahashi, Y. Senba, H. Ohashi, L. G. M. Pettersson, A. Nilsson, and S. Shin, High resolution X-ray emission spectroscopy of liquid water: The observation of two structural motifs, *Chem. Phys. Lett.* 460(4–6), 387 (2008)
9. F. H. Stillinger, Water revisited, *Science* 209(4455), 451 (1980)
10. G. E. Walrafen, Effects of equilibrium H-bond distance and angle changes on Raman intensities from water, *J. Chem. Phys.* 120(10), 4868 (2004)
11. M. Vedamuthu, S. Singh, and G. W. Robinson, Properties of liquid water: Origin of the density anomalies, *J. Phys. Chem.* 98(9), 2222 (1994)
12. R. Bukowski, K. Szalewicz, G. C. Groenenboom, and A. van der Avoird, Prediction of the properties of water from first principles, *Science* 315(5816), 1249 (2007)
13. B. Guillot, A reappraisal of what we have learnt during three decades of computer simulations on water, *J. Mol. Liq.* 101(1–3), 219 (2002)
14. R. Car and M. Parrinello, Unified approach for molecular dynamics and density-functional theory, *Phys. Rev. Lett.* 55(22), 2471 (1985)
15. J. D. Eaves, J. J. Loparo, C. J. Fecko, S. T. Roberts, A. Tokmakoff, and P. L. Geissler, Hydrogen bonds in liquid water are broken only fleetingly, *Proc. Natl. Acad. Sci. USA* 102(37), 13019 (2005)
16. G. S. Fanourgakis, G. K. Schenter, and S. S. Xantheas, A quantitative account of quantum effects in liquid water, *J. Chem. Phys.* 125(14), 141102 (2006)
17. R. Bukowski, K. Szalewicz, G. C. Groenenboom, and A. Van Der Avoird, Polarizable interaction potential for water from coupled cluster calculations (II): Applications to dimer spectra, virial coefficients, and simulations of liquid water, *J. Chem. Phys.* 128(9), 094314 (2008)
18. F. Paesani, S. Iuchi, and G. A. Voth, Quantum effects in liquid water from an *ab initio*-based polarizable force field, *J. Chem. Phys.* 127(7), 074506 (2007)
19. Y. A. Mantz, B. Chen, and G. J. Martyna, Structural correlations and motifs in liquid water at selected temperatures: ab initio and empirical model predictions, *J. Phys. Chem. B* 110(8), 3540 (2006)
20. A. Nilsson and L. G. M. Pettersson, The structural origin of anomalous properties of liquid water, *Nat. Commun.* 6, 8998 (2015)
21. J. D. Smith, C. D. Cappa, K. R. Wilson, R. C. Cohen, P. L. Geissler, and R. J. Saykally, Unified description of temperature-dependent hydrogen-bond rearrangements in liquid water, *Proc. Natl. Acad. Sci. USA* 102(40), 14171 (2005)
22. J. D. Bernal and R. H. Fowler, A theory of water and ionic solution, with particular reference to hydrogen and hydroxyl ions, *J. Chem. Phys.* 1(8), 515 (1933)
23. A. K. Soper, The quest for the structure of water and aqueous solutions, *J. Phys.: Condens. Matter* 9(13), 2717 (1997)
24. A. K. Soper, The radial distribution functions of water and ice from 220 to 673 K and at pressures up to 400 MPa, *Chem. Phys.* 258(2–3), 121 (2000)
25. S. A. Corcelli and J. L. Skinner, Infrared and Ramute HOD in liquid H_2O and D_2O from 10 to 90 degrees celsius, *J. Phys. Chem. A* 109(28), 6154 (2005)
26. T. S. Carlton, Using heat capacity and compressibility to choose among two-state models of liquid water, *J. Phys. Chem. B* 111(47), 13398 (2007)
27. H. Tanaka, Simple physical model of liquid water, *J. Chem. Phys.* 112(2), 799 (2000)
28. A. Zeidler, P. S. Salmon, H. E. Fischer, J. C. Neuefeind, J. Mike Simonson, and T. E. Markland, Isotope effects in water as investigated by neutron diffraction and path integral molecular dynamics, *J. Phys.: Condens. Matter* 24(28), 284126 (2012)
29. J. C. Dore, M. Garawi, and M. C. Bellissent-Funel, Neutron diffraction studies of the structure of water at ambient temperatures, revisited [a review of past developments and current problems], *Mol. Phys.* 102(19–20), 2015 (2004)
30. M. C. Bellissent-Funel, and L. Bosio, A neutron scattering study of liquid D_2O under pressure and at various temperatures, *J. Chem. Phys.* 102(9), 3727 (1995)
31. J. C. Dore, M. A. M. Sufi, and M. C. Bellissent-Funel, Structural change in D_2O water as a function of temperature: The isochoric temperature derivative function for neutron diffraction, *Phys. Chem. Chem. Phys.* 2(8), 1599 (2000)
32. A. K. Soper, The radial distribution functions of water as derived from radiation total scattering experiments: Is there anything we can say for sure? *ISRN Phys. Chem.* 2013, 1 (2013)
33. P. Postorino, M. A. Ricci, and A. K. Soper, Water above its boiling point: Study of the temperature and density dependence of the partial pair correlation functions (I): Neutron diffraction experiment, *J. Chem. Phys.* 101(5), 4123 (1994)
34. K. Amann-Winkel, M. C. Bellissent-Funel, L. E. Bove, T. Loerting, A. Nilsson, A. Paciaroni, D. Schlesinger, and L. Skinner, X-ray and neutron scattering of water, *Chem. Rev.* 116(13), 7570 (2016)
35. L. B. Skinner, C. Huang, D. Schlesinger, L. G. M. Pettersson, A. Nilsson, and C. J. Benmore, Benchmark oxygen-oxygen pair-distribution function of ambient water from X-ray diffraction measurements with a wide Q-range, *J. Chem. Phys.* 138(7), 074506 (2013)
36. J. Morgan and B. E. Warren, X-ray analysis of the structure of water, *J. Chem. Phys.* 6(11), 666 (1938)

37. H. Ohtaki, T. Radnai, and T. Yamaguchi, Structure of water under subcritical and supercritical conditions studied by solution X-ray diffraction, *Chem. Soc. Rev.* 26(1), 41 (1997)
38. J. M. Sorenson, G. Hura, R. M. Glaeser, and T. Head-Gordon, What can X-ray scattering tell us about the radial distribution functions of water? *J. Chem. Phys.* 113(20), 9149 (2000)
39. C. Huang, T. M. Weiss, D. Nordlund, K. T. Wikfeldt, L. G. M. Pettersson, and A. Nilsson, Increasing correlation length in bulk supercooled H_2O, D_2O, and NaCl solution determined from small angle X-ray scattering, *J. Chem. Phys.* 133(13), 134504 (2010)
40. F. N. Keutsch and R. J. Saykally, Water clusters: Untangling the mysteries of the liquid, one molecule at a time, *Proc. Natl. Acad. Sci. USA* 98(19), 10533 (2001)
41. K. A. Tay and F. Bresme, Kinetics of hydrogen-bond rearrangements in bulk water, *Phys. Chem. Chem. Phys.* 11(2), 409 (2009)
42. R. Laenen, C. Rauscher, and A. Laubereau, Dynamics of local substructures in water observed by ultrafast infrared hole burning, *Phys. Rev. Lett.* 80(12), 2622 (1998)
43. R. H. Henchman and S. J. Irudayam, Topological hydrogen-bond definition to characterize the structure and dynamics of liquid water, *J. Phys. Chem. B* 114(50), 16792 (2010)
44. H. J. Bakker and J. L. Skinner, Vibrational spectroscopy as a probe of structure and dynamics in liquid water, *Chem. Rev.* 110(3), 1498 (2010)
45. K. Ramasesha, S. T. Roberts, R. A. Nicodemus, A. Mandal, and A. Tokmakoff, Ultrafast 2D IR anisotropy of water reveals reorientation during hydrogen-bond switching, *J. Chem. Phys.* 135(5), 054509 (2011)
46. R. Kumar, J. R. Schmidt, and J. L. Skinner, Hydrogen bonding definitions and dynamics in liquid water, *J. Chem. Phys.* 126(20), 204107 (2007)
47. F. Perakis, L. D. Marco, A. Shalit, F. Tang, Z. R. Kann, T. D. Kühne, R. Torre, M. Bonn, and Y. Nagata, Vibrational spectroscopy and dynamics of water, *Chem. Rev.* 116(13), 7590 (2016)
48. T. Fransson, Y. Harada, N. Kosugi, N. A. Besley, B. Winter, J. J. Rehr, L. G. M. Pettersson, and A. Nilsson, X-ray and electron spectroscopy of water, *Chem. Rev.* 116(13), 7551 (2016)
49. Ph. Wernet, D. Nordlund, U. Bergmann, M. Cavalleri, M. Odelius, H. Ogasawara, L. Å. Näslund, T. K. Hirsch, L. Ojamäe, P. Glatzel, L. G. M. Pettersson, and A. Nilsson, The structure of the first coordination shell in liquid water, *Science* 304(5673), 995 (2004)
50. J. A. Sellberg, S. Kaya, V. H. Segtnan, C. Chen, T. Tyliszczak, H. Ogasawara, D. Nordlund, L. G. M. Pettersson, and A. Nilsson, Comparison of X-ray absorption spectra between water and ice: New ice data with low pre-edge absorption cross-section, *J. Chem. Phys.* 141(3), 034507 (2014)
51. B. Hetényi, F. De Angelis, P. Giannozzi, and R. Car, Calculation of near-edge X-ray-absorption fine structure at finite temperatures: Spectral signatures of hydrogen bond breaking in liquid water, *J. Chem. Phys.* 120(18), 8632 (2004)
52. T. Head-Gordon and M. E. Johnson, Tetrahedral structure or chains for liquid water, *Proc. Natl. Acad. Sci. USA* 103(21), 7973 (2006)
53. L. Kong, X. Wu, and R. Car, Roles of quantum nuclei and inhomogeneous screening in the X-ray absorption spectra of water and ice, *Phys. Rev. B* 86(13), 134203 (2012)
54. J. D. Smith, C. D. Cappa, B. M. Messer, W. S. Drisdell, R. C. Cohen, and R. J. Saykally, Probing the local structure of liquid water by X-ray absorption spectroscopy, *J. Phys. Chem. B* 110(40), 20038 (2006)
55. W. Chen, X. Wu, and R. Car, X-ray absorption signatures of the molecular environment in water and ice, *Phys. Rev. Lett.* 105(1), 017802 (2010)
56. D. Prendergast and G. Galli, X-ray absorption spectra of water from first principles calculations, *Phys. Rev. Lett.* 96(21), 215502 (2006)
57. T. Fransson, I. Zhovtobriukh, S. Coriani, K. T. Wikfeldt, P. Norman, and L. G. M. Pettersson, Requirements of first-principles calculations of X-ray absorption spectra of liquid water, *Phys. Chem. Chem. Phys.* 18(1), 566 (2016)
58. A. Nilsson, D. Nordlund, I. Waluyo, N. Huang, H. Ogasawara, S. Kaya, U. Bergmann, L. Å. Näslund, H. Öström, P. Wernet, K. J. Andersson, T. Schiros, and L. G. M. Pettersson, X-ray absorption spectroscopy and X-ray Raman scattering of water and ice – An experimental view, *J. Electron Spectrosc. Relat. Phenom.* 177(2–3), 99 (2010)
59. M. Leetmaa, M. P. Ljungberg, A. Lyubartsev, A. Nilsson, and L. G. M. Pettersson, Theoretical approximations to X-ray absorption spectroscopy of liquid water and ice, *J. Electron Spectrosc. Relat. Phenom.* 177(2–3), 135 (2010)
60. J. Vinson, J. J. Kas, F. D. Vila, J. J. Rehr, and E. L. Shirley, Theoretical optical and X-ray spectra of liquid and solid H_2O, *Phys. Rev. B* 85(4), 045101 (2012)
61. O. Fuchs, M. Zharnikov, L. Weinhardt, M. Blum, M. Weigand, Y. Zubavichus, M. Bär, F. Maier, J. D. Denlinger, C. Heske, M. Grunze, and E. Umbach, Isotope and temperature effects in liquid water probed by X-ray absorption and resonant X-ray emission spectroscopy, *Phys. Rev. Lett.* 100(2), 027801 (2008)
62. D. Nordlund, H. Ogasawara, K. J. Andersson, M. Tatarkhanov, M. Salmerón, L. G. M. Pettersson, and A. Nilsson, Sensitivity of X-ray absorption spectroscopy to hydrogen bond topology, *Phys. Rev. B* 80(23), 233404 (2009)

63. S. Kashtanov, A. Augustsson, Y. Luo, J. H. Guo, C. Såthe, J. E. Rubensson, H. Siegbahn, J. Nordgren, and H. Ågren, Local structures of liquid water studied by X-ray emission spectroscopy, *Phys. Rev. B* 69(2), 024201 (2004)

64. J. A. Sellberg, T. A. McQueen, H. Laksmono, S. Schreck, M. Beye, et al., X-ray emission spectroscopy of bulk liquid water in "no-man's land", *J. Chem. Phys.* 142(4), 044505 (2015)

65. M. Odelius, H. Ogasawara, D. Nordlund, O. Fuchs, L. Weinhardt, F. Maier, E. Umbach, C. Heske, Y. Zubavichus, M. Grunze, J. D. Denlinger, L. G. M. Pettersson, and A. Nilsson, Ultrafast core-hole-induced dynamics in water probed by X-ray emission spectroscopy, *Phys. Rev. Lett.* 94(22), 227401 (2005)

66. J. H. Guo, Y. Luo, A. Augustsson, J. E. Rubensson, C. Såthe, H. Ågren, H. Siegbahn, and J. Nordgren, X-ray emission spectroscopy of hydrogen bonding and electronic structure of liquid water, *Phys. Rev. Lett.* 89(13), 137402 (2002)

67. M. Odelius, Molecular dynamics simulations of fine structure in oxygen K-edge X-ray emission spectra of liquid water and ice, *Phys. Rev. B* 79(14), 144204 (2009)

68. L. Weinhardt, O. Fuchs, M. Blum, M. Bär, M. Weigand, J. D. Denlinger, Y. Zubavichus, M. Zharnikov, M. Grunze, C. Heske, and E. Umbach, Resonant X-ray emission spectroscopy of liquid water: Novel instrumentation, high resolution, and the "map" approach, *J. Electron Spectrosc. Relat. Phenom.* 177(2–3), 206 (2010)

69. T. Tokushima, Y. Harada, Y. Horikawa, O. Takahashi, Y. Senba, H. Ohashi, L. G. M. Pettersson, A. Nilsson, and S. Shin, High resolution X-ray emission spectroscopy of water and its assignment based on two structural motifs, *J. Electron Spectrosc. Relat. Phenom.* 177(2–3), 192 (2010)

70. K. M. Lange, M. Soldatov, R. Golnak, M. Gotz, N. Engel, R. Könnecke, J. E. Rubensson, and E. F. Aziz, X-ray emission from pure and dilute H_2O and D_2O in a liquid microjet: Hydrogen bonds and nuclear dynamics, *Phys. Rev. B* 85(15), 155104 (2012)

71. Z. Sun, M. Chen, J. Wang, S. Biswajit, H. Shen, L. Xu, W. Kang, and X. Wu, X-ray absorption of liquid water studied by advanced ab initio methods, *Phys. Rev. B* (Submitted)

72. B. Brena, D. Nordlund, M. Odelius, H. Ogasawara, A. Nilsson, and L. G. M. Pettersson, Ultrafast molecular dissociation of water in ice, *Phys. Rev. Lett.* 93(14), 148302 (2004)

73. M. Neeb, J. E. Rubensson, M. Biermann, and W. Eberhardt, Coherent excitation of vibrational wave functions observed in core hole decay spectra of O_2, N_2 and CO, *J. Electron Spectrosc. Relat. Phenom.* 67(2), 261 (1994)

74. F. Gel'mukhanov, H. Ågren, M. Neeb, J. E. Rubensson, and A. Bringer, Integral properties of channel interference in resonant X-ray scattering, *Phys. Lett. A* 211(2), 101 (1996)

75. M. Odelius, Information content in O[1s] K-edge X-ray emission spectroscopy of liquid water, *J. Phys. Chem. A* 113(29), 8176 (2009)

76. N. A. Besley, Equation of motion coupled cluster theory calculations of the X-ray emission spectroscopy of water, *Chem. Phys. Lett.* 542, 42 (2012)

77. L. Weinhardt, A. Benkert, F. Meyer, M. Blum, R. G. Wilks, W. Yang, M. Bär, F. Reinert, and C. Heske, Nuclear dynamics and spectator effects in resonant inelastic soft X-ray scattering of gas-phase water molecules, *J. Chem. Phys.* 136(14), 144311 (2012)

78. W. Kohn and L. J. Sham, Self-consistent equations including exchange and correlation effects, *Phys. Rev.* 140(4A), A1133 (1965)

79. J. P. Perdew, K. Burke, and M. Ernzerhof, Generalized gradient approximation made simple, *Phys. Rev.* 77, 3865 (1996)

80. P. Giannozzi, S. Baroni, N. Bonini, M. Calandra, R. Car, et al., QUANTUM ESPRESSO: A modular and open-source software project for quantum simulations of materials, *J. Phys.: Condens. Matter* 21(39), 395502 (2009)

81. N. Troullier and J. L. Martins, Efficient pseudopotentials for plane-wave calculations, *Phys. Rev. B* 43(3), 1993 (1991)

82. D. R. Hamann, M. Schlüter, and C. Chiang, Norm-conserving pseudopotentials, *Phys. Rev. Lett.* 43(20), 1494 (1979)

83. D. R. Hamann, Generalized norm-conserving pseudopotentials, *Phys. Rev. B* 40(5), 2980 (1989)

84. J. A. Morrone and R. Car, Nuclear quantum effects in water, *Phys. Rev. Lett.* 101(1), 017801 (2008)

85. G. J. Martyna, M. L. Klein, and M. Tuckerman, Nose–Hoover chains: The canonical ensemble via continuous dynamics, *J. Chem. Phys.* 97(4), 2635 (1992)

86. W. G. Hoover, Canonical dynamics: Equilibrium phase-space distributions, *Phys. Rev. A* 31(3), 1695 (1985)

87. S. Nosé, A unified formulation of the constant temperature molecular dynamics methods, *J. Chem. Phys.* 81(1), 511 (1984)

88. A. Luzar and D. Chandler, Hydrogen-bond kinetics in liquid water, *Nature* 379(6560), 55 (1996)